Electronic Supplementary Information

Quiescent bilayers at the mica-water interface

Francesca Speranza,[a] Georgia A. Pilkington,[a] Thomas G. Dane,[a] Philip T. Cresswell,[a] Peixun Li, [b] Robert M. J. Jacobs,[c] Thomas Arnold,[d] Laurence Bouchenoire,[ef] Robert K. Thomas,[b] and Wuge H. Briscoe*[a]

*[a] School of Chemistry, University of Bristol, Cantock's Close, Bristol BS8 1TS, United Kingdom. Fax: +44 (0)117 925 1295; Tel: +44 (0)117 3318256; [b] Physical and Theoretical Chemistry Laboratory, University of Oxford, South Parks Road, Oxford OX1 3QZ, United Kingdom; [c] Department of Chemistry, Chemistry Research Laboratory, University of Oxford, Mansfield Road, Oxford OX1 3TA, United Kingdom; [d] Diamond Light Source Ltd., Diamond House, Harwell Science and Innovation Campus, Didcot, Oxfordshire, OX11 0DE, UK; [e] XMaS, the UK-CRG, European Synchrotron Radiation Facility (ESRF), 6 Rue Jules Horowitz, BP 220, 38043 Grenoble CEDEX 9, France; [f] Department of Physics, Oliver Lodge Laboratory, University of Liverpool, Oxford Street, Liverpool L69 7ZE, United Kingdom; *E-mail: wuge.briscoe@bris.ac.uk*

A. Experimental and fitted reflectivity curves for C_nTABs

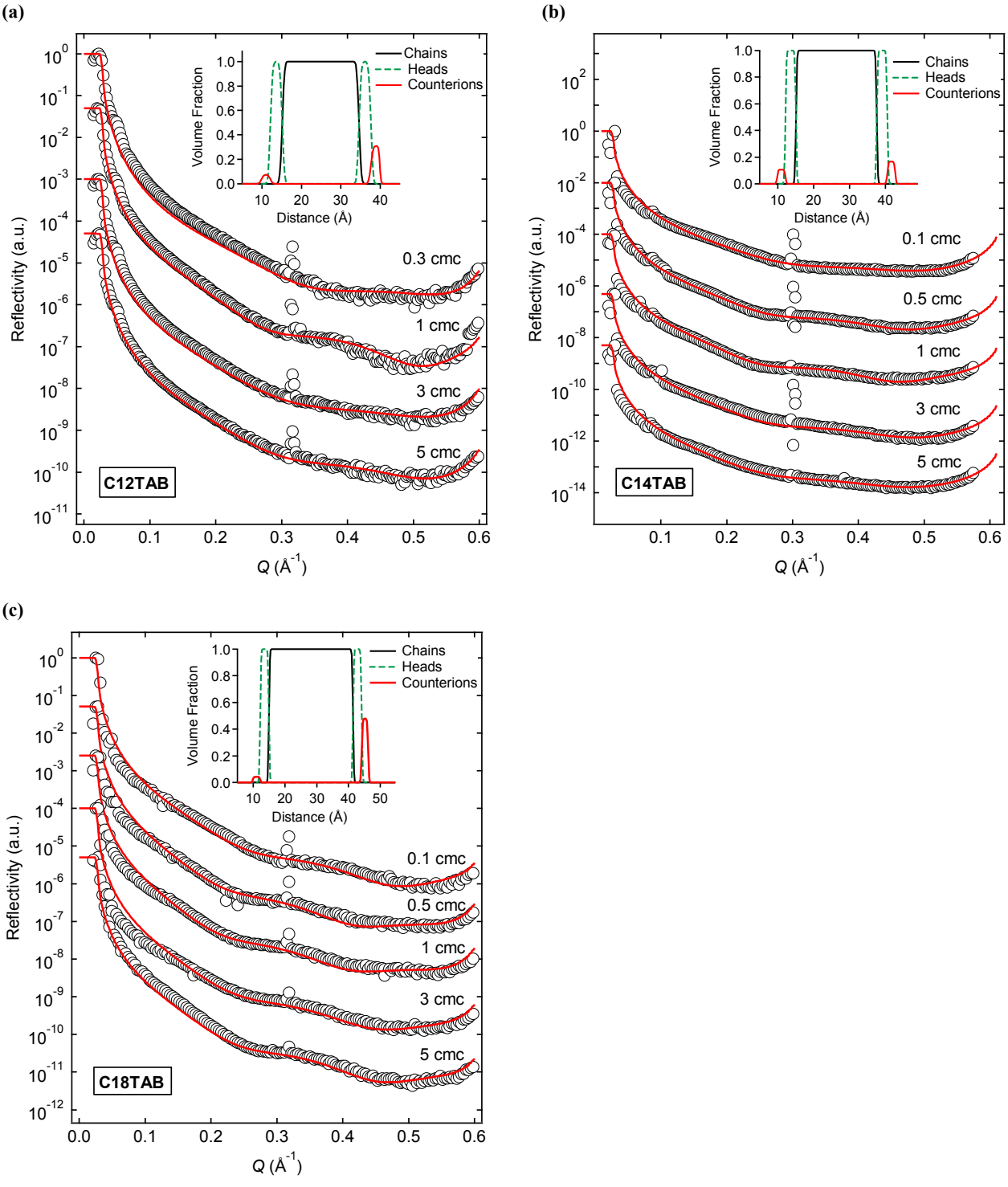

Fig. S1 Experimental (open circles) and fitted (solid curves) reflectivity curves for **(a)** C_{12}TAB, **(b)** C_{14}TAB and **(c)** C_{18}TAB at different concentrations between 0.1 and 5 cmc (as indicated in individual plots). The insets show the volume fractions of different segments at 1 cmc used for the fitting.

B. Fitting parameters for C_nTABs

Surfactant concentration		Inner Headgroup Layer	Outer Headgroup Layer	Alkyl Tail Bilayer	Total Thickness	Roughness at bilayer-water interface (Å)	Coverage (%)
	Tanford's Chain Length $2l_c$ (Å)			33.4			
	Calculated Thickness t_c (Å)	2.2	2.2	29.8	36.6		
0.3 cmc	Fitted Thickness t (Å)	2.3	2.2	16.0	20.5	0.5	56
	Fraction of association (%)	92	57				
	Tilt angle w.r.t. normal			55.9°[#]			
1 cmc	Fitted Thickness t (Å)	2.3	2.3	20.8	25.4	0.9	100
	Fraction of association (%)	87	21				
	Tilt angle w.r.t. normal			46.0°[#]			
3 cmc	Fitted Thickness t (Å)	2.2	2.5	17.5	22.2	0.5	100
	Fraction of association (%)	97	7				
	Tilt angle w.r.t. normal			52.6°[#]			
5 cmc	Fitted Thickness t (Å)	2.3	2.3	18.9	23.5	0.5	100
	Fraction of association (%)	95	16				
	Tilt angle w.r.t. normal			50.0°[#]			

Table S1 Fitting parameters for C_{12}TAB for data shown in Fig. S1(a). ([#]) If tilted bilayers are assumed.

Surfactant concentration		Inner Headgroup Layer	Outer Headgroup Layer	Alkyl Tail Bilayer	Total Thickness	Roughness at bilayer-water interface (Å)	Coverage (%)
	Tanford's Chain Length $2l_c$ (Å)			38.4			
	Calculated Thickness t_c (Å)	2.2	2.2	34.9	41.6		
0.1 cmc	Fitted Thickness t (Å)	2.3	2.2	20.5	25.0	0.5	58
	Fraction of association (%)	100	35				
	Tilt angle w.r.t. normal			53.0°[#]			
0.5 cmc	Fitted Thickness t (Å)	2.4	2.3	22.4	27.1	0.5	70
	Fraction of association (%)	90	36				
	Tilt angle w.r.t. normal			49.3°[#]			
1 cmc	Fitted Thickness t (Å)	2.2	2.3	23.9	28.4	0.5	100
	Fraction of association (%)	45	30				
	Tilt angle w.r.t. normal			46.9°			
3 cmc	Fitted Thickness t (Å)	2.2	2.2	22.4	26.8	0.5	100
	Fraction of association (%)	100	14				
	Tilt angle w.r.t. normal			49.9°[#]			
5 cmc	Fitted Thickness t (Å)	2.2	2.2	22.1	26.5	0.5	100
	Fraction of association (%)	70	10				
	Tilt angle w.r.t. normal			50.4°[#]			

Table S2 Fitting parameters for C_{14}TAB for data shown in Fig. S1(b). ([#]) If tilted bilayers are assumed.

Surfactant concentration		Inner Headgroup Layer	Outer Headgroup Layer	Alkyl Tail Bilayer	Total Thickness	Roughness at bilayer-water interface (Å)	Coverage (%)
	Tanford's Chain Length $2l_c$ (Å)			48.5			
	Calculated Thickness t_c (Å)	2.2	2.2	45.1	50.8		
0.1 cmc	Fitted Thickness t (Å)	2.1	2.2	22.9	27.2	0.5	86
	Fraction of association (%)	100	25				
	Tilt angle w.r.t. normal			57.6°#			
0.5 cmc	Fitted Thickness t (Å)	2.3	2.2	26.6	31.1	0.5	94
	Fraction of association (%)	90	15				
	Tilt angle w.r.t. normal			52.5°#			
1 cmc	Fitted Thickness t (Å)	2.2	2.3	27.7	32.0	0.5	100
	Fraction of association (%)	100	10				
	Tilt angle w.r.t. normal			51.0°#			
3 cmc	Fitted Thickness t (Å)	2.1	2.2	24.7	29.0	0.5	100
	Fraction of association (%)	92	12				
	Tilt angle w.r.t. normal			55.2°#			
5 cmc	Fitted Thickness t (Å)	2.3	2.2	24.2	28.7	0.5	100
	Fraction of association (%)	98	17				
	Tilt angle w.r.t. normal			55.6°#			

Table S3 Fitting parameters for C_{18}TAB for data shown in Fig. S1(c). (#) If tilted bilayers are assumed.

C. Counterion association with the inner and outer quaternary ammonium headgroups for C_nTABs

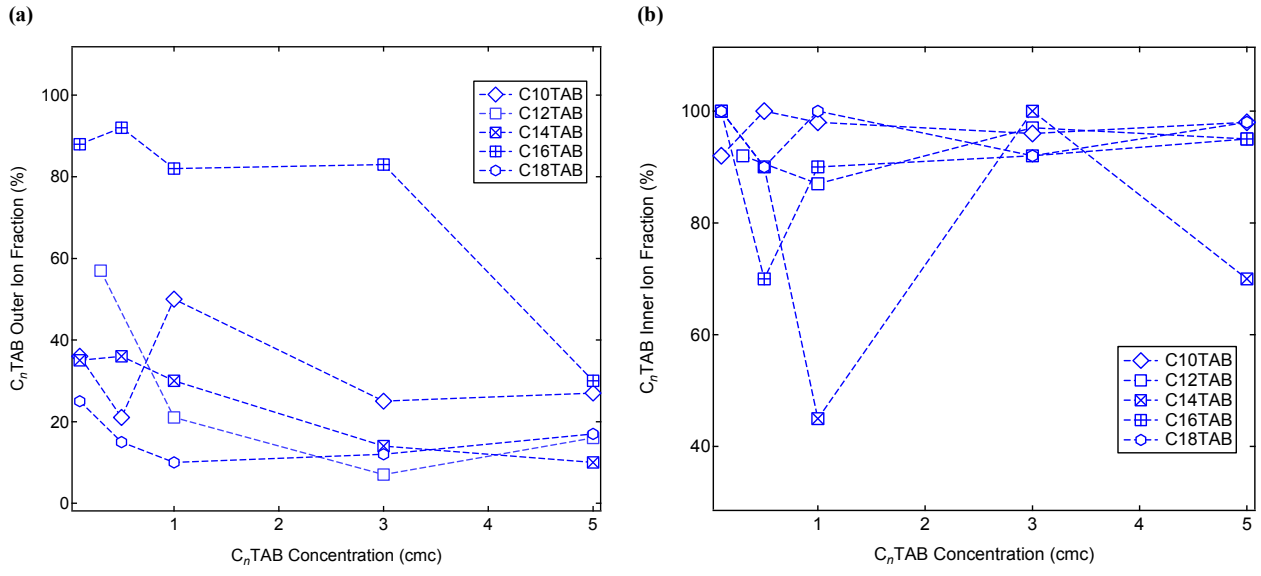

Fig. S3 Fraction of counterions association with **(a)** the inner and **(b)** outer quaternary ammonium headgroups as a function of C_nTABs concentration.

The counterion fraction associated with the inner and outer quaternary ammonium headgroups was also found to vary as a function of C_nTABs concentration (cf. Fig. S3). It is noticeable that the inner and outer surfactant headgroups have different degrees of association. For all the C_nTABs analyzed, the outer headgroups have a smaller degree of association

with the counterions than the inner headgroups at the mica surface. Our results also indicate that the bromide counterions are associated with the inner C_nTABs headgroups and adsorb on the substrate as ion pairs, whereas the potassium ions are associated with the mica which implies that the mica surface charge remains neutral. At present, this remains a limitation of our physical model. For example, a more refined physical model may be to take into consideration of the distribution of potassium counterions dissociated from, and thus in proximity of, the mica surface. However, the volumes and electron densities of bromide and potassium counterions are 28 Å^3 and 21 Å^3, and 0.44 electrons Å^{-3} and 0.48 electrons Å^{-3}, respectively, which are comparable. In particular, C_{14}TAB and C_{16}TAB seem to show anomalous counterion behaviour at ~ 1 cmc and 5 cmc, as shown in Fig. S3, and this point needs further investigation.

As discussed above, the relative errors in the ion fraction are large as compared to other fitting parameters, but this has little effect on the calculated profile of the bilayers, with negligible influence on the results. An important aspect of the sensitivity of X-ray reflectivity to the structure is the resolution of the experiment. In order to fit the subtle features of these counterion distribution accurately, scattering measurements should be performed to sub-Ångström scale resolution. That is, the resolution is ~ $1/Q$, it would thus have been necessary to measure data over a large range of momentum transfer values (Q ~ 10 Å^{-1}) to achieve atomic resolution. However, the Q range in which we have performed the measurements and in which we are interested for our data analysis, *i.e.* in order to fit our bilayer structures, is only from 0 Å^{-1} to the first CTR peak (~ 0.6 Å^{-1}).

D. Experimental and fitted XRR profiles for C_{16}TAB at 1 CMC and calculated XRR profiles assuming different surface coverage and roughness

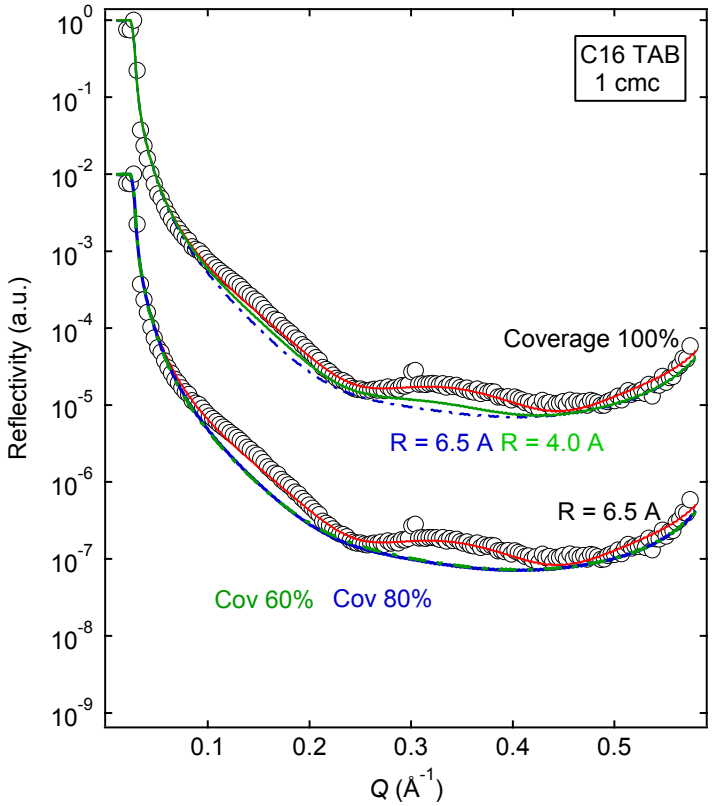

Fig. S4 Experimental (open circles) and fitted (solid red curves) reflectivity curves for C_{16}TAB at 1 cmc using the bilayer model as described in the main text. The top curves show calculated XRR profiles assuming RMS roughness of 6.5 Å (blue dot-dash curve) and 4 Å (green curve), for a surface coverage of 100%. The bottom curves show fitted XRR profiles assuming RMS roughness of 6.5 Å for surface coverage of 60% (green dotted curve) and 80% (blue curve), along with duplicated experimental XRR data for C_{16}TAB at 1 cmc (open circles) but shifted down in the reflectivity for comparison with the calculated profiles.

We have presented the fitting results to our data using a bilayer model in our ms. We have also tried to fit our data with a model that would capture the features of surface aggregates as observed by AFM. A prominent parameter for these surface aggregates is that their surface roughness is much greater than what is required to fit our data. As shown in Fig. 3 (blue curves) and discussed on Page 8 of our ms, relaxing the surface roughness to ~ 6-7 Å (which is the calculated surface roughness for surface cylinders) while keeping the surface coverage by the surfactant tails as 100%, the Kiessig fringes in the calculated profiles are completely damped out, and thus cannot describe the subtle Kiessig fringes in our data. Further relaxing the surface coverage to simulate that reported by AFM imaging would further damp out these

fringes in the calculated profile, as we now show for 60% and 80% surface coverage (lower green and blue curves in Fig. S4). In the figure, we further show that the calculated XRR profile for 100% coverage, and surface roughness of 4 Å (upper green curve) and 6.5 Å (upper blue dot-dash curve) cannot describe our data.